Anal. Chem. **2007,** *79,* 1456−1465

Automated Electric Valve for Electrokinetic Separation in a Networked Microfluidic Chip

Huanchun Cui,[†] Zheng Huang,[§] Prashanta Dutta,[‡] and Cornelius F. Ivory*,[†]

School of Chemical Engineering and Bioengineering and School of Mechanical and Materials Engineering, Washington State University, Pullman, Washington 99164, and Protasis Corporation, 734 Forest Street, Marlboro, Massachusetts 01752

This paper describes an automated electric valve system designed to reduce dispersion and sample loss into a side channel when an electrokinetically mobilized concentration zone passes a T-junction in a networked microfluidic chip. One way to reduce dispersion is to control current streamlines since charged species are driven along them in the absence of electroosmotic flow. Computer simulations demonstrate that dispersion and sample loss can be reduced by applying a constant additional electric field in the side channel to straighten current streamlines in linear electrokinetic flow (zone electrophoresis). This additional electric field was provided by a pair of platinum microelectrodes integrated into the chip in the vicinity of the T-junction. Both simulations and experiments of this electric valve with constant valve voltages were shown to provide unsatisfactory valve performance during nonlinear electrophoresis (isotachophoresis). On the basis of these results, however, an automated electric valve system was developed with improved valve performance. Experiments conducted with this system showed decreased dispersion and increased reproducibility as protein zones isotachophoretically passed the T-junction. Simulations of the automated electric valve offer further support that the desired shape of current streamlines was maintained at the T-junction during isotachophoresis. Valve performance was evaluated at different valve currents based on statistical variance due to dispersion. With the automated control system, two integrated microelectrodes provide an effective way to manipulate current streamlines, thus acting as an electric valve for charged species in electrokinetic separations.

INTRODUCTION

Microfluidic systems integrate different analytical operations such as sample preparation, injection, separation, and detection into a single microdevice.[1] Valving is one of the most important unit operations required for controlling fluid flow inside microchannels. Since the benefits of microfluidic systems were demonstrated in 1993,[2] a number of microvalves have been developed over the past 10 years. Based on the method of actuation, most of these microvalves belong to three major categories: pneumatic,[3,4] phase change,[5,6] and responsive polymers.[7,8] A common characteristic of these microvalves is that they all utilize actuators to physically block the microchannels of interest. The structure of these microvalves is relatively complicated since they require moving parts to close and open the microchannels. Most of microvalves mentioned above were designed to control pressure-driven flow during sample introduction, pumping, and mixing. However these microvalves are limited in use for controlling electrokinetic flow since valve actuation, which usually requires deformation of a polymer layer, heating, cooling, or a buffer pH change, can jeopardize the resolution of electrokinetic separation.

Different flow characteristics require different valve techniques. One way to manipulate electrokinetic driven flow is to control distortion in the current streamlines along which charged species are driven. Ramsey and co-workers[9−14] have developed various valve designs for electrokinetic sample injection and dispensing by manipulating the electric field distribution. Fu and co-workers[15,16] proposed several unique electrokinetic valve configurations for delivering variable-volume sample plugs by controlling the electric field distribution and magnitude within several adjacent channels. All of the examples above represent different schemes

* To whom all correspondence should be addressed. E-mail: cfivory@wsu.edu.
[†] School of Chemical Engineering and Bioengineering, Washington State University.
[§] Protasis Corp.
[‡] School of Mechanical and Materials Engineering.

(1) Vilkner, T.; Janasek, D.; Manz, A. *Anal. Chem.* **2004**, *76*, 3373−3385.
(2) Harrison, D. J.; Fluri, K.; Seiler, K.; Fan, Z. H.; Effenhauser, C. S.; Manz, A. *Science* **1993**, *261*, 895−897.
(3) Unger, M. A.; Chou, H. P.; Thorsen, T.; Scherer, A.; Quake, S. R. *Science* **2000**, *288*, 113−116.
(4) Thorsen, T.; Maerkl, S. J.; Quake, S. R. *Science* **2002**, *298*, 580−584.
(5) Pal, R.; Yang, M.; Johnson, B. N.; Burke, D. T.; Burns, M. A. *Anal. Chem.* **2004**, *76*, 3740−3748.
(6) Chen, Z. Y.; Wang, J.; Qian, S. Z.; Bau, H. H. *Lab Chip* **2005**, *5*, 1277−1285.
(7) Beebe, D. J.; Moore, J. S.; Bauer, J. M.; Yu, Q.; Liu, R. H.; Devadoss, C.; Jo, B. H. *Nature* **2000**, *404*, 588−590.
(8) Luo, Q. Z.; Mutlu, S.; Gianchandani, Y. B.; Svec, F.; Frechet, J. M. J. *Electrophoresis* **2003**, *24*, 3694−3702.
(9) Ermakov, S. V.; Jacobson, S. C.; Ramsey, J. M. *Anal. Chem.* **2000**, *72*, 3512−3517.
(10) Kutter, J. P.; Jacobson, S. C.; Ramsey, J. M. *Anal. Chem.* **1997**, *69*, 5165−5171.
(11) Jacobson, S. C.; Ermakov, S. V.; Ramsey, J. M. *Anal. Chem.* **1999**, *71*, 3273−3276.
(12) Jacobson, S. C.; Ramsey, J. M. *Anal. Chem.* **1997**, *69*, 3212−3217.
(13) Alarie, J. P.; Jacobson, S. C.; Culbertson, C. T.; Ramsey, J. M. *Electrophoresis* **2000**, *21*, 100−106.
(14) Thomas, C. D.; Jacobson, S. C.; Ramsey, J. M. *Anal. Chem.* **2004**, *76*, 6053−6057.
(15) Fu, L. M.; Yang, R. J.; Lee, G. B.; Liu, H. H. *Anal. Chem.* **2002**, *74*, 5084−5091.
(16) Fu, L. M.; Yang, R. J.; Lee, G. B. *Anal. Chem.* **2003**, *75*, 1905−1910.

10.1021/ac061845h CCC: $37.00
Published on Web 01/09/2007

to manipulate the electric field for sample injection in an effort to achieve the sharp sample plug which enables high-resolution separation in zone electrophoresis (ZE). To achieve high resolution in separations, it is also necessary to reduce the dispersion that occurs near T-junctions.

Burns and co-workers[17,18] have successfully developed a method to address this issue by applying shaped electric fields from several pairs of integrated microelectrodes located in the vicinity of an intersection. This method greatly reduced dispersion of DNA bands into side channels while they were being separated by ZE through polyacrylamide gel in the main separation channel. The shaped electric fields were determined primarily on the basis of the electric field applied in the main separation channel. It is relatively easy to find the appropriate shaped electric field for linear electrophoresis, e.g., ZE of DNA since the electric conductivity is homogeneous and the electric field is approximately constant in the main separation channel.

In the case of nonlinear electrophoretic techniques such as isotachophoresis (ITP), it is difficult to find the appropriate electric field for valving since the electrical conductivity is discontinuous and varies as ITP progresses. In this work, we want to address this issue in order to reduce dispersion and sample loss when protein zones pass a T-junction during ITP. This is done using a pair of platinum microelectrodes integrated in the vicinity of the T-junction to act as the electric valve. The positioning of the microelectrodes is similar to that explored by Burns et al.[18]

Determination of the appropriate valve voltages requires knowledge of the local electric field at the T-junction. However, this information is not available during ITP due to transient variations in the local electric field. Instead of manually applying valve voltages, an automated electric valve system has been developed to measure the total current passing through the main separation channel and to automatically inject appropriate valving currents from the microelectrodes based on that measurement. ITP of several fluorescent proteins in free solution was employed to demonstrate and evaluate our valve.

EXPERIMENTAL SECTION

Materials and Reagents. Recombinant green fluorescent protein (GFP, MW ~ 28 000) was obtained from Upstate Biotechnology (Lake Placid, NY). Allophycocyanin (APC, MW ~ 104 000) and *r*-phycoerythrin (PE, MW ~ 240 000) were purchased from Molecular Probes (Eugene, OR). Methylcellulose (MC, viscosity of 2% aqueous solution at 25 °C; 400 cP) and ϵ-amino-*n*-caproic (EACA, MW 131.2) were acquired from Sigma (St. Louis, MO). Hydrochloric acid (HCl, MW 36.5) and tris(hydroxymethyl)-aminomethane (Tris, MW 121.14) were purchased from Fisher Scientific (Fair Lawn, NJ).

Electrolytes and Protein Sample Solution Preparation. The leading electrolyte (LE) solution was prepared by adjusting the 10 mM HCl solution to pH 9.5 with Tris. The terminating electrolyte (TE) solution consists of 60 mM EACA titrated to pH 10.0 with Tris. The proteins PE, GFP, and APC were mixed and diluted in the LE solution. All solutions contain 2% (w/v) MC in order to suppress electroosmotic flow (EOF).

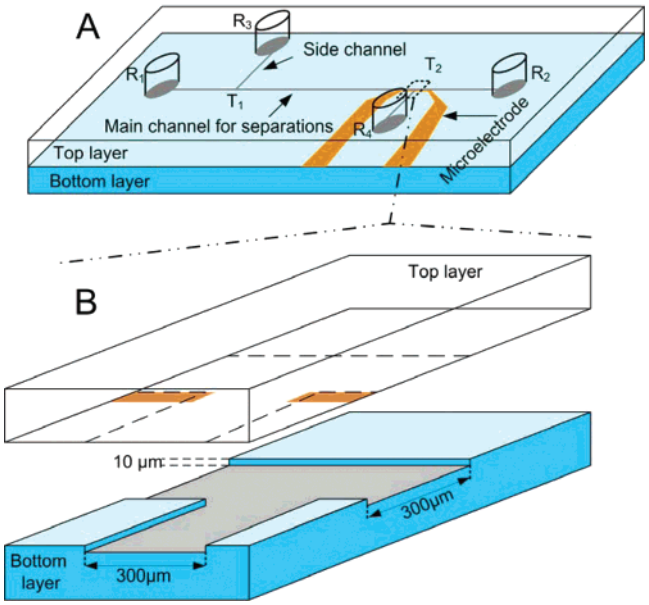

Figure 1. (A) Schematic of the PDMS microfluidic chip used in all electric valve experiments presented in this work. The length of the side channels and the main channel are 5 and 20 mm, respectively. R_1-R_4 are reservoirs and T_1-T_2 are T-junctions. A pair of microelectrodes was fabricated at the vicinity of T_2 for electric valve. (B) Schematic of the junction T_2. The depth and width of the microchannel are 10 and 300 μm, respectively. The pair of microelectrodes was deposited on the bottom surface of the top layer.

Microfluidic Chip Fabrication. A networked poly(dimethylsiloxane) (PDMS) microfluidic chip with a pair of integrated microelectrodes, as shown in Figure 1A, was used in our experiments. The procedure used to fabricate the PDMS chips and the integrated microelectrodes were reported in our previous work.[19, 20] First, a positive pattern of the desired channel structure is formed on a glass substrate using a positive photolithography technique. PDMS prepolymer and curing agent (Sylgard 184, Dow Corning Inc., Midland, MI) are uniformly mixed at a ratio of 10:1, respectively, and degassed for 2 h at 0.001 Torr. The liquid elastomer is cast onto the positive pattern formed on the glass substrate and cured in a hot kiln for 6 h at 80 °C. At the end of the curing process, the elastic polymeric material is carefully peeled from the glass substrate to become the bottom layer of the microchip.

Before this bottom layer is sealed with the top layer, which is a flat PDMS substrate with reservoirs, a pair of microelectrodes is fabricated on the bottom surface of the top layer (Figure 1B) using the following procedure. The bottom surface of the top layer is spin-coated with a highly viscous photoresist, SU-8 2010 (at 1000 rpm for 19 s) and prebaked and then soft-baked at 65 and 95 °C, respectively. The photoresist is then exposed to near-ultraviolet radiation through a mask with a desired pattern of microelectrodes and developed for 60 s in the SU-8 developer (MicroChem Corp., MA). To produce more rigid pattern structures, the patterned photoresist on the bottom surface of the top layer is hard-baked at 115 °C for 150 s. The exposed part of the bottom surface of the

(17) Lin, R. S.; Burke, D. T.; Burns, M. A. *J. Chromatogr., A* **2003**, *1010*, 255–268.
(18) Lin, R. S.; Burke, D. T.; Burns, M. A. *Anal. Chem.* **2005**, *77*, 4338–4347.
(19) Cui, H. C.; Horiuchi, K.; Dutta, P.; Ivory, C. F. *Anal. Chem.* **2005**, *77*, 1303–1309.
(20) Mamun, N. H. A.; Dutta, P. *J. Microlithogr., Microfabr., Microsyst.* **2006**, *5*, 039701.

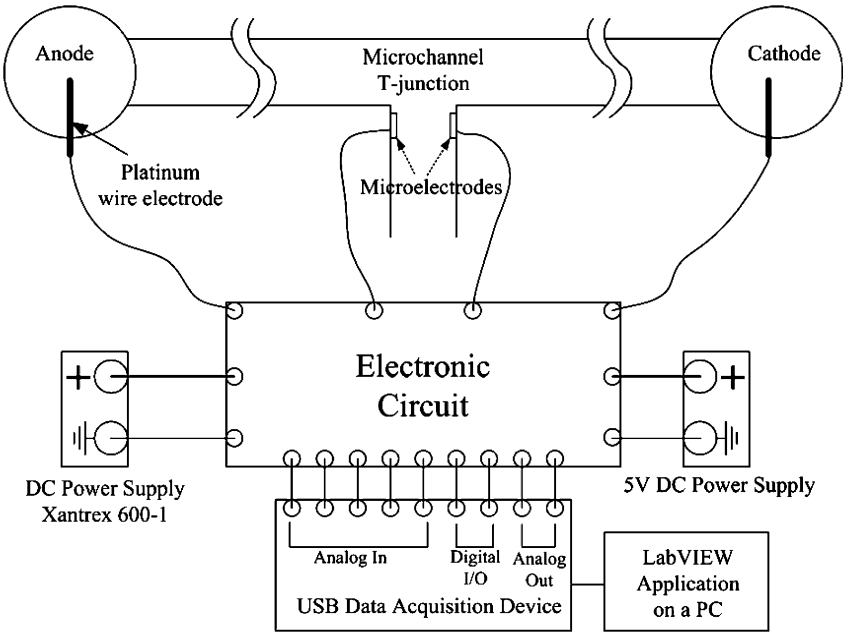

Figure 2. Schematic of the automated electric valve system. The electronic circuit and LabVIEW application were designed in-house. Five "Anolog In", two "Digitial I/O", and two "Analog Out" connections on the USB data acquisition device are used to control the electronic circuit. The DC power supply, Xantrex 600-1, is used to provide 30 V for separation through the platinum wire electrodes as well as to power the electronic circuit. A 5 V DC power supply is used to power several voltage isolation units integrated into the electronic circuit.

top layer is temporarily activated by an RF plasma in the presence of oxygen gas (Plasma Etcher PE 2000, South Bay Technology Inc., San Clemente, CA) to achieve better adhesion between the PDMS surfaces and the metal about to be deposited. The photoresist patterned surface is then sputtered (Edwards Auto 306, BOC Edwards, MA) with a titanium thin film (~30 nm thick) which is followed by a sputtered platinum layer approximately 175 nm thick. The hard-baked photoresist was then stripped off the PDMS surface. The PDMS surface patterned with microelectrodes was then cleaned with acetone, isopropyl alcohol, and DI water. For permanent bonding of the top and bottom layers, both layers were cleaned by oxygen RF plasma (PDC-32G, Harrick Scientific Co., NY). This microfluidic chip (Figure 1) consists of a main channel and two side channels that branch out from the main channel. All channels are 300 μm wide and 10 μm deep.

Automated Control. An electronic circuit (Figure 2) designed in-house has the ability to sense the electric current passing through the main channel and then to supply a specific amount of control current to the two microelectrodes. The circuit was drawn in EAGLE (CadSoft Computer, Delray Beach, FL) software and printed onto a prototype circuit board by AP Circuits (Calgary, AB, Canada). The electronic units including operational amplifiers, transistors, isolation amplifiers, DC−DC converters, resistors, capacitors, and relays were then soldered onto the circuit board. Five analog inputs, two analog outputs, and four digital I/O ports on a data acquisition device (LabJack, Lakewood, CO) were employed to read and send commands to the electronic circuit (Figure 2). The data acquisition device was controlled by software programmed in LabVIEW (National Instruments Corp., Austin, TX). Please note that the electronic circuit (see Supporting Information) was exclusively designed for the purpose of the electric valve, which has the following functions: current/voltage measurement and inject/drain specific amount of current through microelectrodes. The direct use of this design for other applications is not recommended. However, after slight modifications, it can be used to control voltage/current/conductivity sensors that are integrated in a microfluidic chip. But readers should be very careful about the working range of each electronic unit on the board.

Experimental Procedure. The procedure used to run ITP in a networked microfluidic chip was reported in our previous work.[21] Briefly, all channels were pressure-filled with the LE from reservoir R_1 (Figure 1). After all the reservoirs were cleaned by removing excessive LE, 30 μL of LE and a 2% MC solution were loaded into R_1 and R_4, respectively. Protein sample solution was then carefully pressure-filled into the channel from reservoir R_3 at ~5 psi until a drop of liquid appeared at the channel entrance inside reservoir R_2. Reservoir R_2 and R_3 were then cleaned and loaded with 30 μL of TE and 2% MC solution, respectively. Note that the initial buffer distribution varies from experiment to experiment since the volume of protein sample solution loaded by this method is not precisely controlled.

Platinum wire electrodes were immersed in reservoirs R_1 and R_2, while reservoirs R_3 and R_4 were left electrically floating. ITP was carried out at a constant voltage of 30 V supplied by the controller which is powered by an XHR 600-1 power supply (Xantrex Technology Inc, Vancouver, Canada) and a 5 V DC power supply (Allied Electronics, Fort Worth, TX). Microelectrodes integrated in the chip were connected by wire to the controller for the electric valve.

Imaging. The loaded chip was mounted underneath the 4× objective lens of a Leica DMLB fluorescence microscope equipped with a CCD camera (SPOT RT color, Diagnostic Instruments, Inc., Sterling Heights, MI). The fluorescent proteins were excited with a mercury lamp (OSRAM HBO 100 W/2) using a filter cube (DMLB 513804, Leica Microsystems, Inc., IL) and photographs

(21) Cui, H. C.; Dutta, P.; Ivory, C. F. *Electrophoresis*, in press.

were taken by software that controls the CCD camera. The variance of a protein zone is obtained using ImageJ (NIH, Bethesda, MD) with Moment Calculator (http://rsb.info.nih.gov/ij/plugins/moments.html). After subtracting the background signal intensity from an experimental photograph, the protein concentration zone is centered inside a rectangular box for moment analysis. The rectangular box is set so that its lateral edges are just outside the edges of the protein zone, and they extend for 1 mm along the separation channel with the protein zones roughly centered along this axis.

Simulation. The Nernst−Planck physics built into Femlab (COMSOL, Burlington, MA) was employed to perform two-dimensional simulations of linear and nonlinear electrophoresis, ZE and ITP, respectively, in a microchannel with a T-junction.

Under an external electric field, each charged species in a solution migrates by diffusion, electromigration, and convection. The flux of each species is given by the equation

$$\mathbf{N}_i = -D_i \nabla C_i - z_i F \mu_i C_i \nabla \mathbf{\Phi} + C_i \mathbf{u} \qquad (1)$$

Here, $\mathbf{N}_i$ is the flux of species i, C_i is the concentration of species i, z_i is the charge, F is the faraday constant, μ_i is the ion mobility, Φ is the electric potential, D_i is the diffusion coefficient, and $\mathbf{u}$ is the bulk flow velocity.

Each species is governed by the mass conservation law expressed as follows:

$$\frac{\partial C_i}{\partial t} = -\nabla \cdot \mathbf{N}_i \qquad (2)$$

Some assumptions are made in the simulations. The sources that induce bulk flows such as pressure differences among the reservoirs and EOF due to the methyl-cellulose-coated surface charges[19] are neglected, and thus the bulk flow velocity, $\mathbf{u}$, in eq 1 is assumed to be zero.

A constant electric potential was set between boundaries b_1 and b_2 (Figure 3). In the case of the electric valve with constant valving voltages, two additional constant voltages were set on boundaries b_3 and b_4 (Figure 3B). In the case of the automatic electric valve, the total current was calculated by integrating the current density along boundary b_2 and a fixed percentage of the total current was assigned in the form of current densities along boundaries b_3 and b_4. All channel walls are impermeable to the current and to migrating species.

RESULTS AND DISCUSSION

Control Current Streamlines Using Integrated Microelectrodes. A simulation result (Figure 3A) shows that the uncontrolled current streamlines bend into the side channel as they pass through a T-junction.[22] The bent current streamlines are the primary source of dispersion of a concentration zone of charged species since it is driven along the current streamlines. An obvious way to reduce this type of dispersion is to block the side channel entrance. However this requires actuation of a physical barrier which complicates microfluidic chip fabrication as well as experimental operation. Another way to reduce such dispersion is to manipulate the current streamlines by applying additional electric fields in the vicinity of the T-junction. If the current streamlines in the separation channel are straightened by the additional electric field, then dispersion would not be expected to occur since charged species follow the current streamlines.

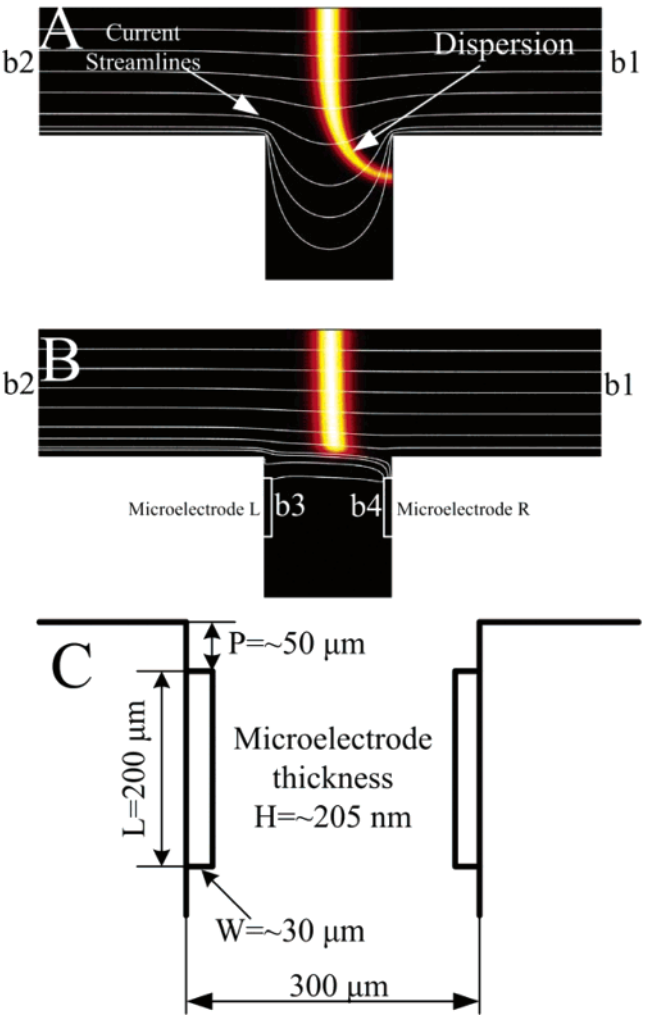

Figure 3. (A) Simulated images showing dispersion of a concentration zone and bent current streamlines at a T-junction. (B) Simulation of an electric valve showing greatly reduced dispersion and straightened current streamlines. (C) Schematic of microelectrode positions at the T-junction. *P* is the distance between the microelectrode and the main channel. *L*, *W*, and *H* represent the length, width, and thickness of the microelectrode, respectively. The position of the microelectrode differs slightly from chip to chip. The following statement is applied to all the simulation results presented in this paper: The simulated image is only the middle part of the whole computing domain, which has a 2 mm long main channel and a 0.5 mm long side channel branched out from the middle of the main channel. All concentration zones are negatively charged and migrate to the left (the anode). All channels in the simulated images are 300 μm wide.

The concentration zone in Figure 3B shows almost no dispersion due to the straightened current streamlines. The two microelectrodes used to control the current streamline act as a virtual valve which not only prevents losses into the side channel but also greatly reduces dispersion of the concentration zone. Since neutral species do not migrate along the current streamlines, this virtual valve exclusively controls the charged species, the targets of electrophoresis.

(22) Cui, H. C.; Horiuchi, K.; Dutta, P.; Ivory, C. F. *Anal. Chem.* **2005**, *77*, 7878−7886.

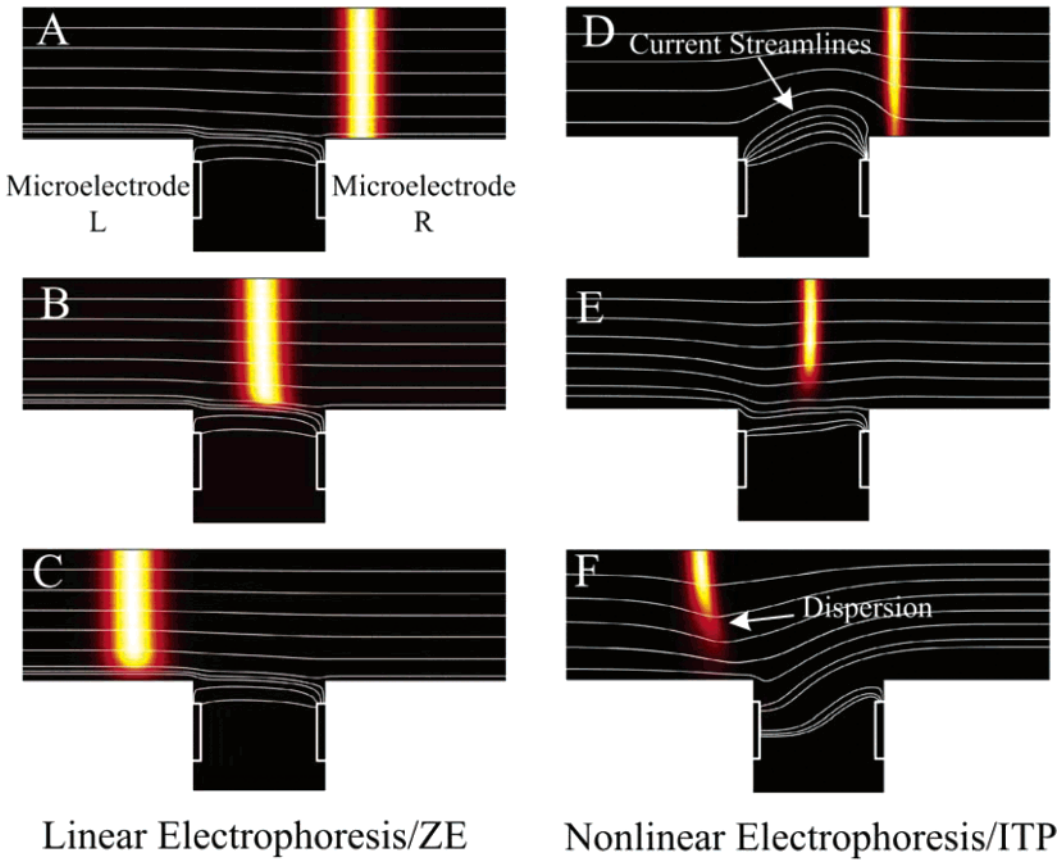

Figure 4. Simulation results for an electric valve under both linear electrophoresis and nonlinear electrophoresis using constant electric valve voltages. Linear electrophoresis/ZE: 100 V along the main channel, 60 V at microelectrode L, and 45 V at microelectrodes R. Nonlinear electrophoresis/ITP: 100 V along the main channel, 95 V at microelectrode L and 80 V at microelectrode R. See Figure 3 for the description of the whole computing domain and simulated images.

Microelectrode Design Concerns. The valve voltages applied to the microelectrodes depend on the position and size of the microelectrodes as well as the local electric field around the T-junction. The positioning and sizing of the microelectrodes were experimentally investigated by Burns and co-workers[18] in an effort to obtain minimal mass loss into the side channel. There are concerns about electrode erosion and electrolysis when the current density on a microelectrode is too high. To avoid electrode erosion and electrolysis, the microelectrodes need to be large and thick. To make the microelectrodes larger, they are extended in length (L) instead of width (W) (Figure 3C) to make the side channel more accessible. To avoid contact between the microelectrodes and the concentration zone, the microelectrodes are located 50 μm away from the main channel. With the size and the position shown in Figure 3C, no bubble formation due to electrolysis was found in experiments and only some minor electrode erosion was observed after multiple runs.

Electric Valve with Constant Valve Voltages. Once the size and position of each microelectrode is fixed, the valve voltages only depend on the local electric field. Therefore, the valve voltages need not vary in the case of a linear electrokinetic flow since the local electric field remains approximately unchanged due to the homogeneous background buffer ion which dominates the local conductivity. The simulation (Figure 4A−C) of an electric valve for linear electrokinetic flow (ZE) with constant valve voltages reveals that the current streamlines remain straight and unchanged before, during, and after the concentration zone passes the T-junction. Therefore, using an electric valve for linear electrokinetic flow is effective when constant valve voltages are applied.

However, an electric valve with a constant valve voltage is not expected to work effectively for nonlinear electrokinetic flows, and our simulation (Figure 4D−F) confirms that the shape of the current streamlines changes dramatically as nonlinear electrophoresis (ITP) progresses. In our simulation, constant valve voltages were intentionally chosen in the simulation to have straight current streamlines at the moment when the concentration zone approaches the middle of the T-junction (Figure 4E). However, after the concentration zone passed the T-junction, the lower part of it tilted clockwise due to the skewed current streamlines (Figure 4F).

It is relatively easy to choose appropriate valve voltages in the modeling since the local electric field around the T-junction can be analyzed in the simulations. However, it is difficult to comprehensively measure and analyze the local electric field during the experiments. Furthermore, variation of the initial buffer and sample distribution from experiment to experiment makes it more difficult to adjust the valve voltages on the basis of the results of previous experiments. The experimental result shown in Figure 5 is one of only a few successful runs among tens of experiments performed with constant valve voltages. A series of photographs shown in Figure 5A−D demonstrate how three adjacent protein

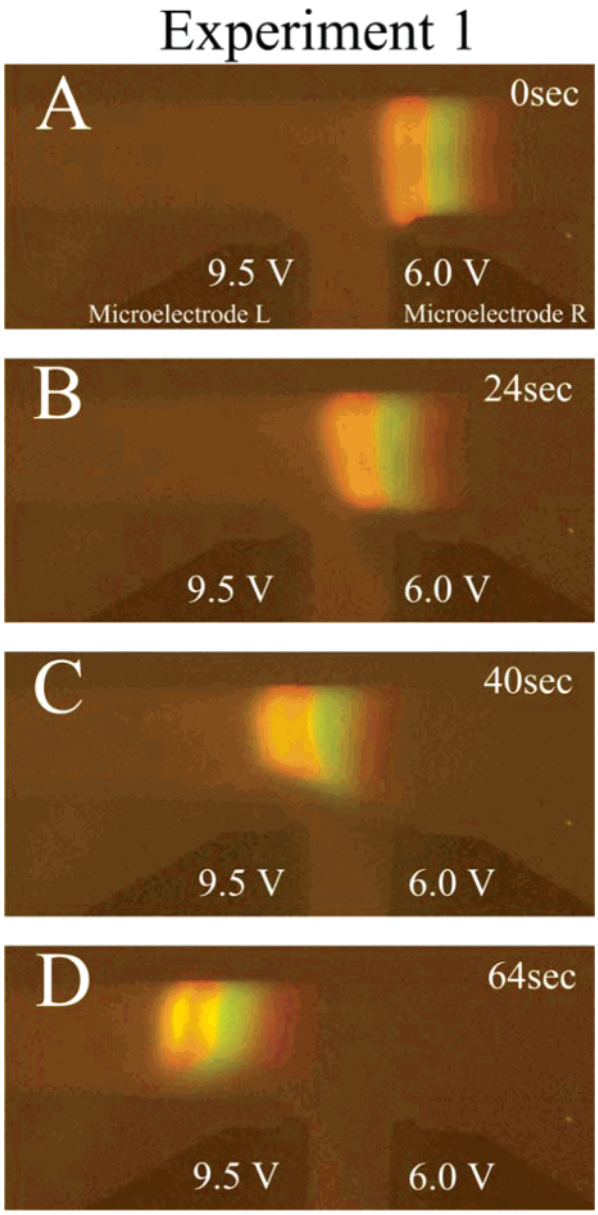

Figure 5. Electric valve experiment with constant valve voltages. Time-series photos A−D of ITP near a T-junction were captured at junction T_2 as shown in Figure 1A. Valve voltages of 9.5 and 6.0 V were applied to the left and right microelectrodes, respectively. The initial sample solution consisted of PE (0.04 μg/μL), GFP (0.06 μg/μL), and APC (0.06 μg/μL). The three protein zones from left to right are PE, GFP, and APC.

zones maneuvered through the T-junction with two fixed valve voltages of 9.5 and 6.0 V applied to microelectrodes R and L, respectively.

In this case, the protein zones were nicely formed as they approached the T-junction (Figure 5A). As they migrated into the T-junction, they skewed slightly and no expansion of their lower part into the T-junction was observed (Figure 5B). Parts C and D of Figure 5 show that the protein zones "jumped" across the T-junction with the lower part of it skewing behind the center of mass of the peak before jumping and then skewing ahead. Although no protein loss into the side channel was experimentally observed, the protein zones were dispersed when passing the T-junction, and the reproducibility of this result is very low due to the difficulties mentioned above.

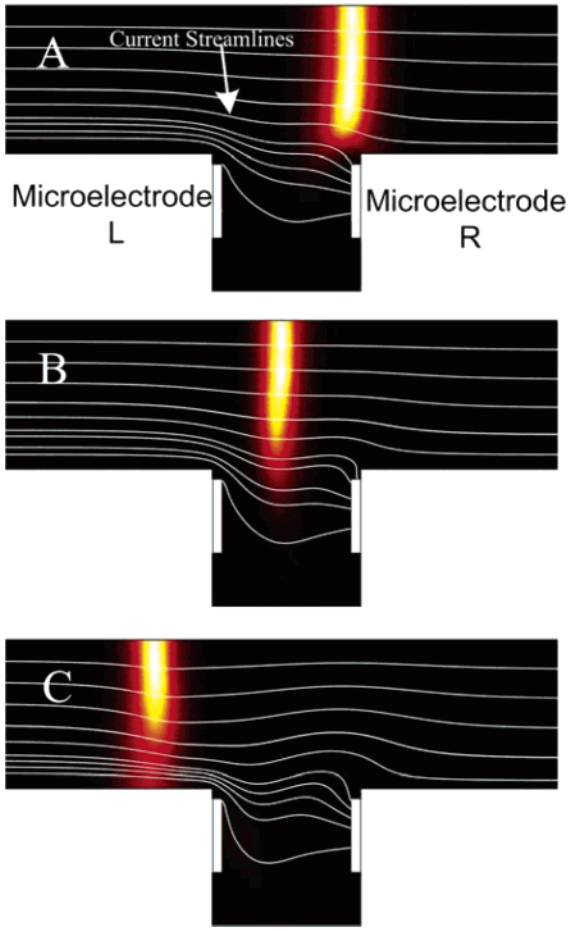

Figure 6. Simulation of automated electric valve as an ITP zone passes a T-junction. See Figure 3 for the description of the whole computing domain and simulated images. The total current was automatically calculated in the simulation by integrating the current density along the left boundary of the main channel (b_2 as shown in Figure 3A). Of the total current 18% flowed from microelectrode L into the channel, and 58% of total current flowed from the channel onto microelectrode R. Along the main channel, 30 V was applied.

Developing an Automated Electric Valve. To increase the reproducibility and further reduce dispersion, the valve voltages must change in response to the variation of the local electric field in the T-junction. Another microelectrode positioned at the point where the centerline of the side channel crosses the upper wall of the main channel might be used as a voltage sensor to provide the information on the variation of the local electric field. However, integration of such a voltage sensor certainly complicates the design, especially when considering large-scale integration of multiple electric valves. Instead of relying on the additional microelectrode to sense the local electric field and then control the valve voltages, an electronic system was developed to control the electric currents carried on the pair of microelectrodes on the basis of the total current passing through the main channel, which can be measured outside of the microfluidic chip. The following paragraph details the development of the automated electric valve system.

As ITP progresses, the total current passing through the main channel decreases because an increasing length of the channel is occupied by the low conductivity TE. Ideally, the valve voltages that straighten the current streamlines in a T-junction at any given

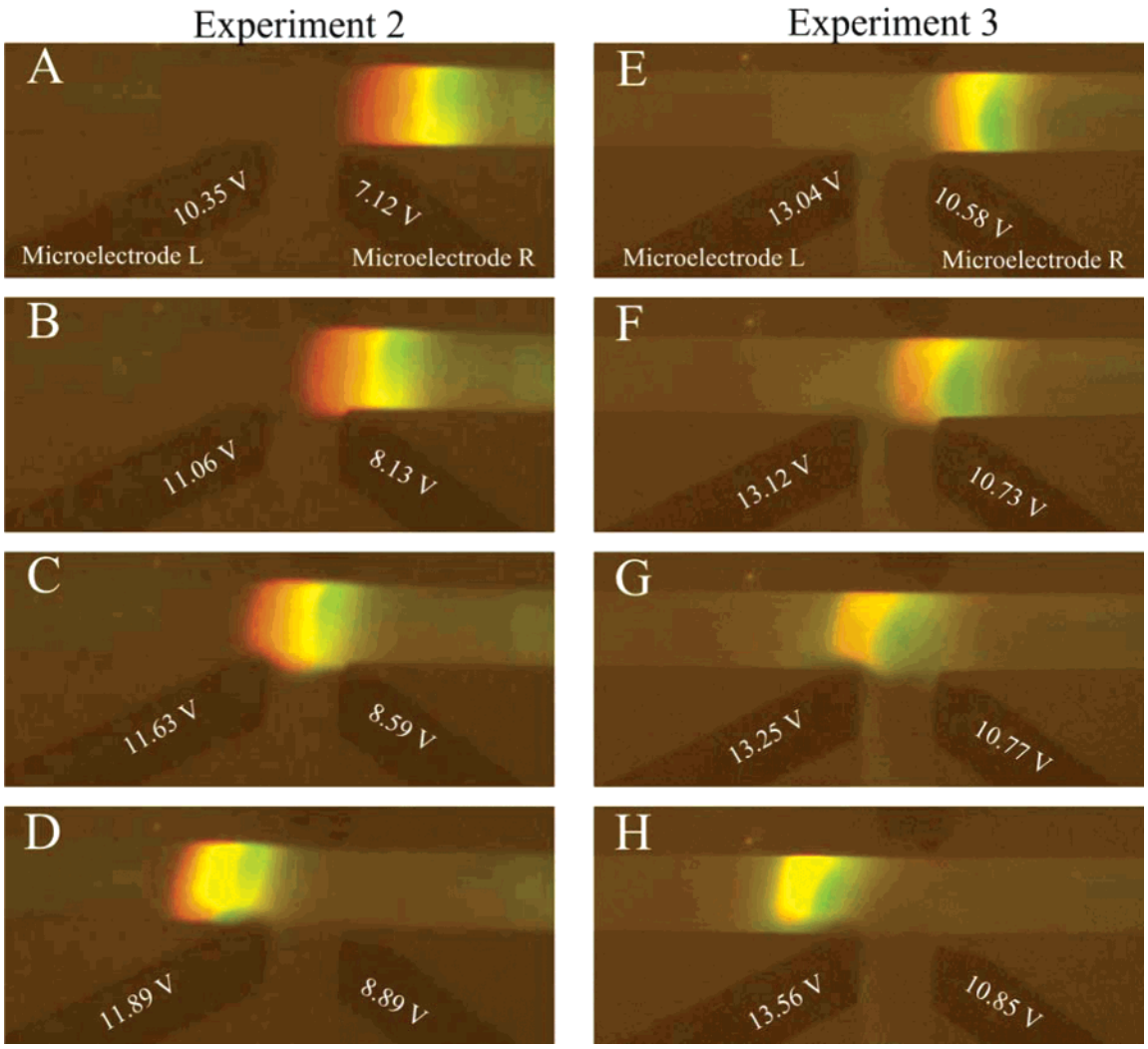

Figure 7. Automated electric valve experiments with different initial protein sample concentrations and initial buffer distributions. Both experiments were performed in the same chip. Both experiments had 15−17% of the total current flowed from microelectrode L into the channel and 38−40% of the total current flowed from the channel onto microelectrode R. Experiment 2: the initial sample solution consisted of PE (0.06 μg/μL) and GFP (0.06 μg/μL). Experiment 3: the initial sample solution consisted of PE (0.03 μg/μL) and GFP (0.05 μg/μL). The resulting valve voltages at each moment are indicated on the microelectrodes.

moment during ITP should exist, but it is difficult to find them because of a lack of knowledge of the local electric field during these experiments. However, knowledge of the total current is available because it can be easily measured. Since any valve voltage applied to an electrode should generate a corresponding valve current, the appropriate valve voltages can be chosen on the basis of the knowledge of the total current if the relationship between the valve current and the total current is known. Therefore, the problem turns out to be finding the appropriate valve currents applied to the pair of microelectrodes to make the total current go straight through the T-junction. If the positions and size of the microelectrodes are fixed, the valve currents only depend on the total current. Although the relationship between the two is elusive, the assumption that the valve currents are a fixed percentage of the total current makes the relationship straightforward. On the basis of this assumption, an automated electric valve system has been developed which measures the total current every 30 ms and assigns a certain amount of current to the microelectrodes. The ratios of the valve currents on the pair of microelectrodes to the total current are crucial to valve performance and need to be experimentally determined. Despite the variation of initial buffer distribution and sample concentration from experiment to experiment, the automated electric valve system is expected to work properly with the determined ratios unless the position and size of the microelectrodes are changed.

Simulation and Experimental Demonstration of Automated Electric Valve. The simulation results shown in Figure 6 demonstrate that an automated electric valve, based on the assumption made above, can significantly improve valve performance. In this simulation, 18% of total current flowed from microelectrode L into the channel and 58% of total current flowed from the channel onto microelectrode R. Only slight changes in the shape of the current streamlines (Figure 6A−C) were observed in this simulation as the ITP concentration zone passed the T-junction, so the dispersion which occurred in the lower part of the ITP concentration zone (Figure 6C) is negligible and no sign of mass loss into the side channel was witnessed in the simulation. Despite the fact that the current streamlines around the T-junction are not perfectly straight, the strategy that application of fixed percentages of the total current to the pair of

microelectrodes is effective enough to provide high-quality valving. With the electronic control system, experimental operations became automatic and straightforward and experimental results became reproducible. To obtain optimum valve performance, only two parameters (the ratios of two valve currents to the total current) need to be adjusted in the homemade LabVIEW program which controls the electronic circuit.

The following two experiments shown in Figure 7 demonstrate the benefits of the automated electric valve system. Experiments 2 and 3 are two independent runs performed in the same microfluidic chip and under the same experimental conditions except that they have different initial buffer distributions and sample concentrations. Of the total current 15−17% goes from microelectrode L into the channel, while 38−40% of the total current goes from the channel onto microelectrode R. The difference in the breadth of the protein zones in experiments 2 and 3 (Figure 7) is due to their different initial sample concentrations. Despite such differences, the protein zones in both experiments followed very similar paths when passing the T-junction. Although there was a small jump in the protein zones near the left corner of the T-junction (Figure 7C,G) in both experiments, the intensity of the jump was greatly reduced when compared to the experiment shown in Figure 5, in which the valve voltages were constant. To understand why this happened, it is necessary to examine the resulting valve voltages on the pair of microelectrodes which were automatically recorded in the LabVIEW application. For example, the valve voltages in experiment 2 shown in Figure 7A−D increased gradually from 10.35 to 11.89 V on microelectrode L and from 7.12 to 8.89 V on microelectrode R. This increase is the response to the change of the local electric field in an effort to maintain the shape of the current streamlines. The valve voltages on the pair of microelectrodes in experiment 2 (Figure 7A−D) are different from those in experiment 3 (Figure 7E−H) primarily because of the different initial buffer distributions and initial sample concentrations. It is very unlikely that an operator could apply the appropriate valve voltages without the help of an automatic control system because of the variation in the initial experimental conditions.

Figure 8 is a data plot of the valve currents, the total current, and the valve voltages recorded in another experiment that was performed in the same chip as that shown in Figure 7. The automated electric valve was turned on for about 20 min. During this period, the protein zones approached and passed the junction T_2 (Figure 1A) and continuously migrated toward the anode reservoir until it approached the junction T_1 (Figure 1A). Figure 8A shows that, as expected, the total current gradually decreased from ~1.0 to ~0.4 μA as ITP progressed. The corresponding valve currents also shown in Figure 8A are 15−17% of the total current on microelectrode L and 38−40% of total current on microelectrode R. The gap between the two vertical lines (Figure 8) indicates the length of time that the protein zones took to pass the T-junction. The resulting valve voltages are shown in Figure 8B. The valve voltages reached the peak right after the protein zones passed the T-junction and decreased as they migrated further away from the T-junction. The total current, valve current, and the valve voltages stayed constant (not shown in Figure 8) after the ITP concentration zones entered the anode reservoir because the whole channel was occupied by uniform TE buffer

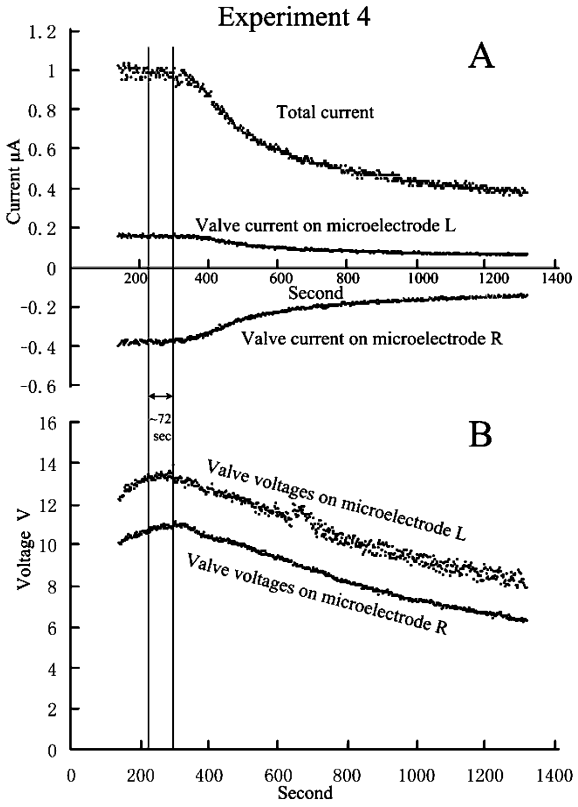

Figure 8. Variation of the total current, valve currents, and valve voltages with time. The automated electric valve system was turned on before the ITP concentration zone approached junction T_2 as shown in Figure 1A and was not turned off until the ITP concentration zone approached junction T_1 as also shown in Figure 1A. Of the total current 15−17% flowed from microelectrode L into the channel, and 38−40% of total current flowed from the channel onto microelectrode R. Two vertical lines indicate the time period during which the ITP concentration zone was passing the T-junction.

and the local electric field around the T-junction no longer changed.

Performance Evaluation of Automated Electric Valve. Valve performance can be evaluated in terms of dispersion and sample loss at a T-junction. Since no obvious sample loss into the side channel was observed in our experiments, the valve performance was evaluated only by the dispersion. The dispersion of a protein zone is quantified by its variance. The method used to obtain the variance of a protein zone is mentioned in the Experimental Section. The initial variance is defined as the variance of the protein zones before entering the junction area. Experiments with different valve currents were employed to evaluate the valve performance. These experiments (Figure 9) were performed in the same chip with the same sample concentration. Please note that the chips employed in these experiments have slightly different microelectrode positions from the chips used in those experiments shown in Figure 5 and Figure 7. This difference in the microelectrode positions was introduced during the fabrication step, where the top layer of the PDMS substrate containing the pair of microelectrodes was manually aligned to the bottom substrate that contains channels before bonding.

Experiment 5 (Figure 9A−D) differs from experiment 6 (Figure 9E−H) by the percentage of the total current that flows from microelectrode L into the channel. Parts A and E of Figure

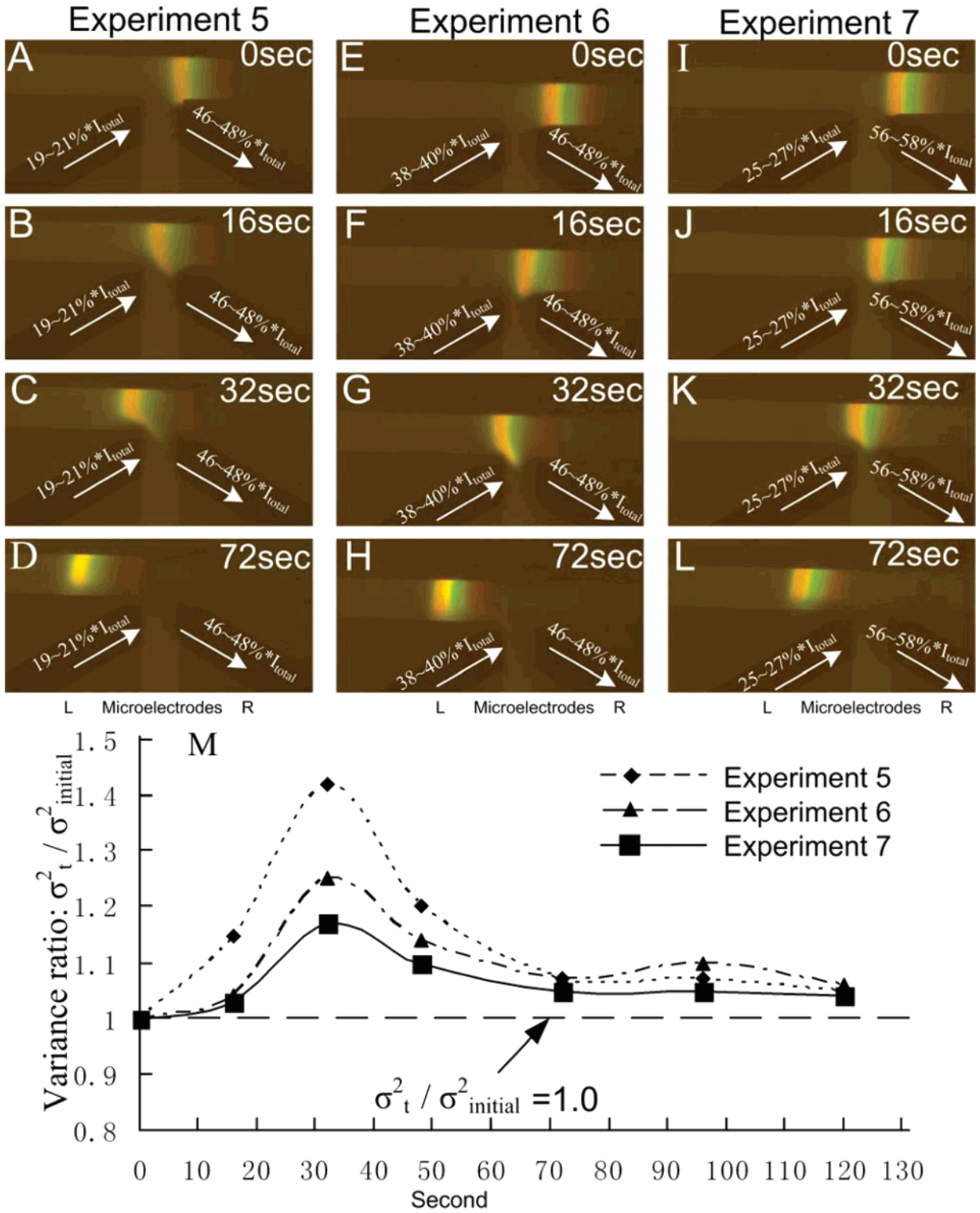

Figure 9. Evaluation of valve performance based on the variance ratios of dispersion at different valve currents. The percentages of the total current (e.g., 19−21%I_{total}) are indicated on the microelectrodes, and the arrows indicate the direction of the valve currents. Photographs A−L correspond to the variance ratios plotted in M. The corresponding photographs of other points plotted in M were not shown. The initial sample concentration in all experiments consisted of PE (0.03 μg/μL), GFP (0.06 μg/μL), and APC (0.06 μg/μL).

9 show that the protein zones in both experiments were similar and well-formed when approaching the T-junction. As they migrated further into the T-junction, the ITP concentration zone shown in Figure 9B was slightly dispersed, while the counterpart in Figure 9F maintained its shape. The comparison of dispersion was quantified in Figure 9M, which revealed that, at $t = 16$ s, the variance ratio ($\sigma_t^2/\sigma_{initial}^2$) in experiment 5 reached 1.15 while it stayed close to 1.0 in experiment 6.

To explain why the protein zones behaved differently in experiments 5 and 6, it is necessary to emphasize the fact that all the proteins were negatively charged and thus they are attracted to the anode. The potential on an anode increases as more applied

current flows out from it. The increased potential makes the anode more attractive to the negatively charged proteins. On the other hand, the potential on a cathode decreases as more current flows into it, and thus it repels the negative charged proteins more strongly. Since microelectrode L supplied a higher percentage of total current into channel in experiment 6 than in experiment 5, it was relatively more anodic in experiment 6. Therefore, the dispersion that occurred in experiment 5 (Figure 9B) was greatly reduced in experiment 6 (Figure 9F) because the lower part of the protein zones was straightened by the stronger attraction toward microelectrode L. For the same reason, the lower part of the protein zones jumped over the left corner of the T-junction in experiment 5 (Figure 9C), while the counterpart in experiment 6 (Figure 9G) climbed over the left corner. The corresponding variance ratio at this moment (32 s) increased to 1.42 and 1.25 for experiments 5 and 6, respectively (Figure 9M). After the protein zones passed the T-junction (Figure 9D,H), dispersion was greatly reduced due to the well-known self-sharpening ability of ITP. This was also demonstrated in Figure 9M in terms of the intensity of the variance ratio, which dropped quickly in both experiments after the protein zones passed by the T-junction and stayed very closely to 1.0 as they migrated further away from the T-junction.

Although the valve performance was greatly improved in experiment 6 when compared to that in experiment 5, there was still room for improvement. For example, the dispersion which occurrs near the left corner of the T-junction in experiment 6 can potentially be reduced. This dispersion happened because microelectrode L excessively attracted the lower part of the protein zones and pulled it down into the side channel more than 50 μm. Experiment 7 was designed to reduce this type of dispersion by further adjusting the valve currents. To prevent the lower part of the ITP zone from entering the side channel, it has to be pushed up vertically by the joint repelling force from both microelectrodes. To do so, the valve currents used in experiment 7 decreased on microelectrode L and increased on microelectrode R when compared to those in experiment 6. Parts I−L of Figure 9 clearly demonstrated that the dispersion was further reduced during the ITP zone passing by the T-junction because the lower part of the ITP concentration was successfully prevented from entering the side channel. Figure 9M also confirms that the protein zones were least dispersed in experiment 7 on the basis of the variance ratio.

CONCLUSION

An automatically controlled electric valve system has been demonstrated in a microfluidic chip with T-junctions as a means of reducing dispersion and sample loss into side channels during nonlinear electrophoresis (ITP) of proteins. The dispersion and sample loss at a T-junction is primarily due to the deformation of current streamlines as current passes through the T-junction. Simulation results clearly demonstrated that the current streamlines bent by a T-junction in linear electrokinetic electrophoresis can be straightened by applying constant valve voltages onto a pair of microelectrodes that were appropriately positioned along the side channel walls. However, both simulation and experimental results confirm that constant valve voltages were not able to produce satisfactory valve performance for isotachophoretic concentration zones passing a T-junction due to the variation of the local electric field as ITP progresses.

To optimize valve performance, the valve voltages must automatically change in response to the variation of the local electric field during ITP. This was accomplished by using an electronic control system that was developed to measure the total current passing through the main channel and to automatically assign a specific amount of valve current to the pair of microelectrodes. The simulation of the automated valve strategy proves that the shape of the current streamlines maintains very well and the valve performance was greatly improved as the concentration zone passes a T-junction. Experiments with an automated electric valve system showed excellent valve performance and dramatically improved reproducibility. Experiments also demonstrated that the behavior of protein zones when passing a T-junction can be manipulated by carefully adjusting the valve currents. Comparison of the variance ratio of protein zones provides an effective way to evaluate the valve performance.

The automated electric valve system provides a robust and simple method for controlling current streamlines and reducing dispersion at T-junctions during nonlinear electrophoresis. This system can be easily expanded to provide automated electric valves for a microfluidic chip with multiple T-junctions. Eventually, it is expected that the automated electric valve units will be incorporated into large-scale microfluidic network as virtual valves for electrokinetic flow.

ACKNOWLEDGMENT

This material is based upon work supported by the National Science Foundation under Grant No. CTS-0300802. The use of the bright field fluorescence microscope, provided by the Center for Multiphase Environmental Research (CMER) at Washington State University, is gratefully acknowledged.

SUPPORTING INFORMATION AVAILABLE

Image of electronic circuit in Figure 2 and a movie. This material is available free of charge via the Internet at http://pubs.acs.org.

Received for review October 1, 2006. Accepted November 17, 2006.

AC061845H